

A nitrogen sensitive model of leaf carbon dioxide and water vapour gas exchange: application to 13 key species from differently managed mountain grassland ecosystems

Georg Wohlfahrt ^{a,b,*}, Michael Bahn ^a, Ingrid Horak ^a, Ulrike Tappeiner ^a,
Alexander Cernusca ^a

^a *Institut für Botanik, Universität Innsbruck, Sternwartestr. 15, A-6020 Innsbruck, Austria*

^b *Centro di Ecologia Alpina, Viote del Bondone, 38404 Trento, Italy*

Abstract

During the EU-project ECOMONT (Project No. ENV4-CT95-0179), which focuses on effects of land-use changes on mountain ecosystems, an experimental and modelling strategy at the leaf level was developed, which centres on the intimate relationship between leaf nitrogen content and net photosynthesis. Leaf nitrogen content reflects nutrient availability, shows characteristic seasonal dynamics and is of great importance for the analysis of intraspecific variability of gas exchange. The fully parameterised leaf model is capable of predicting net photosynthesis and stomatal conductance for any combination of microclimatic variables as well as any leaf nitrogen content. At the ECOMONT pilot research area Monte Bondone (Trentino/Italy) three grassland sites differing in land-use, a hay meadow, a pasture and an area abandoned since 35 years were selected as study sites. Leaf gas exchange characteristics and nitrogen contents of 13 species were studied and used for parameterising nitrogen sensitive leaf models. Independent data sets, diurnal courses of photosynthesis and stomatal conductance under the prevailing environmental conditions, were used for validation. A sensitivity analysis was performed in order to test the ability of the model to account for changes in leaf nitrogen content, varying leaf nitrogen content together with the environmental driving variables. These leaf models provide the physiological basis for scaling-up gas exchange from the leaf to the whole plant and canopy level and further to the landscape level. © 1998 Elsevier Science B.V. All rights reserved.

Keywords: Model; Leaf gas exchange; Nitrogen; Land-use; Mixed grassland

1. Introduction

During the EU-TERI-project ECOMONT (Project No. ENV4-CT95-0179; Cernusca et al., 1996), which aims at studying the effects of land-use changes on mountain ecosystems in major

* Corresponding author. Tel.: +43 512 5075917; fax: +43 512 5072975; e-mail: georg.wohlfahrt@uibk.ac.at

mountain regions of Europe, special emphasis was laid on differently managed grassland ecosystems (Cernusca et al., 1998, this issue), which are characterised by a very high diversity of plant species (Cernusca et al., 1992; Tappeiner et al., 1998, this issue; Tasser et al., 1998). These semi-natural grassland ecosystems represent early stages in old field succession initiated by cessation of intensive management (hay making and grazing), progressing to the climax stage, a mixed evergreen/deciduous forest (Cernusca et al., 1992; Pedrotti, 1995). At the ECOMONT pilot research area Monte Bondone (Trentino/Italy), three sites differing in type and intensity of management, a hay meadow, mowed once a year, a pasture, grazed by cattle and horses and an area abandoned since 35 years were selected.

Land-use changes are characterised by shifting resource ratios (e.g. the ratio between nutrient and light availability; Tilman, 1988, 1994; Bahn et al., 1994; Tappeiner and Cernusca, 1994). To evaluate the effects of land-use changes on gas exchange, we have thus chosen leaf nitrogen content as a key variable. Leaf nitrogen content is one of the most important factors determining plant photosynthetic performance (Evans, 1989), which has led other researchers (Harley et al., 1992; Friend, 1995; Leuning et al., 1995; Ninemets and Tenhunen, 1997) to account in their modelling efforts for the effects of changes in leaf nitrogen content. Leaf nitrogen content moreover reflects nutrient availability (Chapin, 1980; Bahn et al., 1994), shows characteristic seasonal dynamics (Mooney et al., 1981) and is of great value for the analysis of intraspecific variability of gas exchange (Bassow and Bazzaz, 1997).

To be representative in predicting gas exchange of these species-rich canopies, it was necessary to establish a solid physiological data basis for as many species as possible and to apply this information by the means of a model characterised by a high responsiveness to a parameter altered due to land-use changes, such as leaf nitrogen content. Since the leaf level represents the basis for scaling up gas exchange from the leaf to the whole plant and canopy level and further to the landscape level in a bottom-up approach (Baldocchi, 1993), the above mentioned is especially important, in

order to maintain a sensitivity to these parameters also at higher levels in the modelling hierarchy (Reynolds et al., 1996). In the following a combined experimental and modelling approach is presented and applied to 13 key species of three differently managed mountain grassland ecosystems.

2. Methods

2.1. Sites and investigated species

Field investigations were carried out during the summers of 1993, 1996 and 1997 in the Southern Alps on the Monte Bondone plateau (Trentino/Italy, latitude 46°01'20" N, longitude 11°02'30" E) at an elevation between 1500–1600 m above sea level. The mean annual temperature is 5.5°C, ranging from –2.7°C in January to 14.4°C in July (Gandolfo and Sulli, 1993). Precipitation is abundant throughout the whole year (1189 mm), with two peaks in June (132 mm) and October (142 mm) and a minimum of 53 mm in January (Gandolfo and Sulli, 1993).

Three sites, differing in land-use, were investigated: A hay meadow, mowed once a year, a pasture, grazed by cattle and horses and an area abandoned since 35 years. A general characterisation of the different sites is given in Table 1.

Criteria for the selection of the investigated species were high abundance and/or major contribution to stand biomass on either one of the sites (species typical for a special site), or on all of the sites (species of overall importance for the vegetation types of the Monte Bondone study area). According to these criteria eight herbs (*Plantago atrata*, *Plantago media*, *Polygonum viviparum*, *Potentilla aurea*, *Rhinanthus alectorolophus*, *Trifolium montanum*, *Trifolium pratense* and *Trollius europaeus*), four grasses (*Dactylis glomerata*, *Koeleria pyramidata*, *Nardus stricta* and *Trisetum flavescens*) and one dwarf shrub (*Vaccinium myrtillus*) were selected. Since the upper leaves (> 30 cm) of *T. europaeus* showed visible signs of senescence already during June, when the lower leaves were fully developed, we decided to treat the lower, fully developed, leaves and the upper, al-

Table 1
General characterisation of the investigated sites at the Monte Bondone study area

	Meadow	Pasture	Abandoned area
Elevation (m a.s.l.)	1550	1560	1550
Exposition	E	E	SE
Inclination (°)	3	5	6
Management	Mowed	Grazed	Abandoned since 35 years
Vegetation type	Polygono–Trisetion	Siversio–Nardetum strictae	Siversio–Nardetum strictae ^b
Maximum canopy height (cm)	80	16	30
Soil type ^{a,c}	Cambisol with mull	Cambisol with mull	Cambisol with mull
Soil depth (cm) ^a	75	42	60
Rooting depth (cm) ^a	20	13	20
Soil water storage capacity (mm) ^a	340	242	309

Data from Tappeiner and Cernusca 1994, except for: ^a ... Neuwinger and Hofer, unpublished; ^b ... dominated by dwarf shrubs; and ^c ... FAO-classification.

ready senescent, leaves separately in order to account for these distinct phenological differences. *P. atrata*, *P. viviparum*, *P. aurea* and *T. europaeus* are species that are equally highly abundant on all of the investigated sites. *K. pyramidata*, *T. montanum* and *P. media* are species typical for the pasture, *D. glomerata*, *T. pratense*, *T. flavescens* and *R. alectorolophus* are typical for the meadow and *N. stricta* and *V. myrtilus* are typical for the abandoned area. All of the selected species are perennials, except for *R. alectorolophus*, which is an annual species.

2.2. Experimental methods

To reach the aims defined in the introduction we followed an experimental strategy combining four different types of measurements (see also Bahn and Cernusca, 1998):

1. Single factor response curves of net photosynthesis and stomatal conductance, which were conducted on a limited number of leaves on that particular site, where each species occurs at its optimum, in order to establish the parameters required for the photosynthesis submodel.

2. Episodical measurements throughout the vegetation period of net photosynthesis and stomatal conductance under the prevailing environmental conditions, in order to obtain the parameters required for the stomatal conductance submodel.

3. Episodical measurements throughout the vegetation period of photosynthetic capacity, on a greater number of leaves for each key species, in order to establish the nitrogen dependencies of photosynthetic capacity and consequently of the three main component processes of net photosynthesis (see below). Photosynthetic capacity (A_{\max} ; for a list of abbreviations and symbols refer to Appendix A) is defined as the net photosynthetic rate at saturating light intensity, ambient CO_2 partial pressure and air humidity and a leaf temperature of 20°C.

4. Diurnal courses of photosynthesis and stomatal conductance under the prevailing environmental conditions in order to validate the leaf models.

A_{\max} may be considered a key parameter of gas exchange for several reasons. Firstly, it is likely that A_{\max} is determined by RUBISCO activity (Ögren, 1993; Ögren and Evans, 1993), which makes it possible to estimate V_{cmax} , the maximum rate of carboxylation from measured A_{\max} . V_{cmax} in turn is strongly correlated to J_{max} , the maximum rate of electron transport (Wullschlegel, 1993; Leuning, 1997) and to R_{dark} , the dark respiration rate (Walters and Field, 1987; Ceulemans and Saugier, 1991). Therefore measurements of A_{\max} can be used to derive estimates of the key parameters of the leaf model at 20°C. Secondly, there exists a strong correlation between A_{\max} and leaf nitrogen content (N_L ; Field and Mooney, 1986; Evans, 1989), which provides the possibility

to explicitly incorporate nitrogen dependencies of V_{cmax} , P_{ml} and R_{day} . Thirdly, A_{max} was also measured when taking response curves of photosynthesis to light, CO_2 and humidity, thus representing a logical interface to the response curves. Finally A_{max} is a readily measurable parameter enabling us to investigate a greater number of leaves per species, which allows for an assessment of intraspecific variability of photosynthetic performance.

Response curves were conducted on *D. glomerata* (1993, 1996), *N. stricta* (1996), *P. atrata* (1996), *P. viviparum* (1996), *R. alectorolophus* (1993), *T. pratense* (1993), *T. flavescens* (1993, 1996) and *T. europaeus* (1996) using two $\text{CO}_2/\text{H}_2\text{O}$ porometers (Heinz WALZ GmbH, Effeltrich, Germany) together with the cuvettes PMK-10 and GK-0235P of the same origin. This equipment was modified to allow for automatic controlling of photosynthetic photon flux density, leaf temperature, air vapour pressure and CO_2 partial pressure. In addition, in 1996 another fully climatized $\text{CO}_2/\text{H}_2\text{O}$ porometer (CIRAS-1, PP-Systems, Hitchin Herts, UK) was used for response curves on *D. glomerata*, *K. pyramidata*, *P. media*, *P. viviparum*, *P. aurea*, *T. montanum*, *T. flavescens*, *T. europaeus* and *V. myrtillus*.

CO_2 response curves (referred to as A/C_i curves in the following) were conducted at a photosynthetic photon flux density of approx. $1200 \mu\text{mol}/\text{m}^2$ per s by stepwise increasing CO_2 partial pressure from 7 to 100 Pa, light response curves were conducted at an ambient CO_2 partial pressure of 35 Pa by stepwise decreasing photosynthetic photon flux density from 1200 to $0 \mu\text{mol}/\text{m}^2$ per s and humidity response curves were conducted at a photosynthetic photon flux density of approx. $1200 \mu\text{mol}/\text{m}^2$ per s and an ambient CO_2 partial pressure of 35 Pa by stepwise decreasing air vapour pressure at a constant leaf temperature of 20°C from ambient humidity to approx. 0.3 kPa. A/C_i curves and light response curves were conducted at an average ambient humidity of approx. 1 kPa and leaf temperatures between $5\text{--}30^\circ\text{C}$. One–seven leaves, with typically 3–5 steps per leaf, were investigated for each type of response curve and leaf temperature level.

For measurements of net photosynthesis and stomatal conductance under the prevailing environmental conditions and of photosynthetic capacity in 1996 and 1997 two portable $\text{CO}_2/\text{H}_2\text{O}$ porometers (CIRAS-1, PP-Systems, Hitchin Herts, UK and LCA-3, ADC Ltd., Hoddesdon, Herts, UK) were used.

Calculations of net photosynthetic rate, stomatal conductance, transpiration rate and internal CO_2 partial pressure were made using the equations of von Caemmerer and Farquhar (1981). All gas exchange rates are described on the basis of the projected leaf area, except for *N. stricta*, whose gas exchange rates are expressed on a surface area basis, because of its uniform circular leaf shape and its leaf orientation, which is more or less perpendicular to the ground surface.

The leaf area inside the cuvettes was measured using a leaf area meter (CI-203, CID Inc., Vancouver, USA). All measured leaves were collected, oven dried at 70°C for at least 72 h and weighed (AE-260, Mettler Instrumente AG, Greifensee–Zürich, Switzerland). Total leaf nitrogen was measured using an elemental analyser (CHNS-932, LECO Instruments, Kirchheim, Germany).

2.3. Leaf gas exchange model

The widely used, mechanistically based Farquhar model (Farquhar et al., 1980; von Caemmerer and Farquhar, 1981) of carbon assimilation of C_3 plants, modified according to Harley and Tenhunen (1991), was employed. Essential to this model is that CO_2 uptake is either entirely limited by RUBISCO activity and the respective partial pressures of the competing gases CO_2 and O_2 at the sites of carboxylation (W_C) or by electron transport (W_J), which limits the rate at which RuBP is regenerated. Limitations of RuBP regeneration arising from the availability of inorganic phosphate (P_i) for photophosphorylation (W_P ; Sharkey, 1985) are not considered in the present approach. Net photosynthesis A may then be expressed as

$$A = \left(1 - \frac{0.5 \cdot O}{\tau \cdot C_i}\right) \cdot \min\{W_C, W_J\} - R_{\text{day}} \quad (1)$$

where O and C_i are the partial pressures of O_2 and CO_2 in the intercellular space, respectively. τ is the specificity factor for RUBISCO (Jordan and Ogren, 1984), R_{day} is the rate of CO_2 evolution from processes other than photorespiration and $\min\{\}$ denotes ‘the minimum of’.

R_{day} is assumed to be a proportion of the dark respiration rate, R_{dark} , mediated by I_{fac} , a dimensionless coefficient representing the degree to which R_{dark} is inhibited in the light according to

$$R_{\text{day}} = I_{\text{fac}} \cdot R_{\text{dark}} \quad (2)$$

I_{fac} and thus the extent to which R_{dark} is inhibited in the light, depends on light intensity according to Falge et al. (1996)

$$I_{\text{fac}} = 0.5 \quad \text{if } \text{PPFD} > 25 \mu\text{mol/m}^2 \text{ per s} \quad (3a)$$

$$I_{\text{fac}} = k \cdot \text{PPFD} + d \quad \text{if } \text{PPFD} \leq 25 \mu\text{mol/m}^2 \text{ per s} \quad (3b)$$

where $k = -0.02$ ($\text{m}^2\text{s}/\mu\text{mol}$) and $d = 1$ ($-$).

The carboxylation rate limited solely by the amount, activation state and kinetic properties of RUBISCO and the respective partial pressures of the competing gases CO_2 and O_2 at the sites of carboxylation is given by

$$W_C = \frac{V_{\text{cmax}} \cdot C_i}{C_i + K_C \cdot \left(1 + \frac{O}{K_O}\right)} \quad (4)$$

where V_{cmax} is the maximum rate of carboxylation and K_C and K_O are the Michaelis–Menten constants for carboxylation and oxygenation, respectively.

The rate of carboxylation limited solely by the rate of RuBP regeneration due to electron transport, W_J , is given by

$$W_J = \frac{P_m}{1 + \frac{O}{\tau \cdot C_i}} \quad (5)$$

where P_m is the CO_2 saturated rate of photosynthesis at any given irradiance and temperature (for a detailed discussion of P_m see Harley and Tenhunen, 1991). This expression of W_J is equivalent to that used by Farquhar and von Caemmerer (1982), if their parameter J is equal to $4 P_m$.

P_m is expressed as a light dependency using the equation by Smith (1937) from Harley and Tenhunen (1991)

$$P_m = \frac{\alpha \cdot \text{PPFD}}{\left(1 + \frac{\alpha^2 \cdot \text{PPFD}^2}{P_{\text{ml}}^2}\right)^{0.5}} \quad (6)$$

where α is the initial slope of the curve relating CO_2 saturated net photosynthesis to irradiance (on an incident light basis) and P_{ml} is the potential rate of RuBP regeneration.

V_{cmax} and P_{ml} depend upon temperature and, given their optimum response to temperature (Harley and Tenhunen, 1991; Leuning, 1997), are described using the equation by Johnson et al. (1942), normalised to a reference temperature (293.16 K) as in Leuning (1997).

Parameter

$$\text{Parameter}(T_{\text{ref}}) \cdot \exp\left[\frac{\Delta H_a}{R \cdot T_{\text{ref}}} \cdot \left(1 - \frac{T_{\text{ref}}}{T_K}\right)\right] \\ = \frac{\text{Parameter}(T_{\text{ref}}) \cdot \exp\left[\frac{\Delta H_a}{R \cdot T_{\text{ref}}} \cdot \left(1 - \frac{T_{\text{ref}}}{T_K}\right)\right]}{1 + \exp\left[\frac{\Delta S \cdot T_K - \Delta H_d}{R \cdot T_K}\right]} \quad (7)$$

Where Parameter is either V_{cmax} or P_{ml} and Parameter (T_{ref}) is the potential value that this parameter would have at the reference temperature in the absence of any deactivation due to high temperature. ΔH_a is the energy of activation, ΔH_d is the energy of deactivation, ΔS is an entropy term, T_K is the leaf temperature in K and R is the gas constant. Note that our interpretation of Parameter (T_{ref}) is different from the one used by Leuning (1997), where Parameter (T_{ref}) is interpreted as the actual value of this parameter at the reference temperature, which is mathematically incorrect, although with little numerical consequences (Leuning, personal communication).

R_{dark} , K_C , K_O increase with temperature, whereas τ is a declining function of temperature (see Harley and Tenhunen, 1991) and their temperature dependencies are each given by:

$$\text{Parameter} = \text{Parameter}(T_{\text{ref}}) \\ \exp\left[\frac{\Delta H_a}{R \cdot T_{\text{ref}}} \cdot \left(1 - \frac{T_{\text{ref}}}{T_K}\right)\right] \quad (8)$$

Table 2

Parameters determining the temperature dependencies, according to Eq. (8), of the RUBISCO specificity factor, τ (from Jordan and Ogren, 1984) and the Michaelis–Menten constants for carboxylation and oxygenation, K_C and K_O (from Badger and Collatz, 1977), respectively

Parameter	Units	τ (–)	Units	K_C (Pa)	K_O (Pa)
Parameter (T_{ref})	—	2838.06	Pa	19.42	12 554.23
ΔH_a	J/mol	–28 990	J/mol	65 000	36 000

which is the same as Eq. (7), with the denominator set to unity. Parameter can be substituted for either R_{dark} , K_C , K_O or τ . Parameter (T_{ref}), in this case, is the actual rate at the reference temperature.

To be able to predict gas exchange at the leaf level, the photosynthesis model has to be combined with a model predicting stomatal conductance (Harley and Tenhunen, 1991). For this purpose the empirical model by Ball et al. (1987), modified according to Falge et al. (1996), was chosen

$$g_s = g_{min} + G_{fac} \cdot (A + I_{fac} \cdot R_{dark}) \cdot 10^2 \cdot \frac{hs}{C_s} \quad (9)$$

where g_s is the stomatal conductance, g_{min} is the minimum or residual stomatal conductance and hs and C_s are the relative humidity (as a decimal fraction) and the CO_2 partial pressure at the leaf surface. The factor 10^2 corrects for the differences in the units of g_s and g_{min} and $(A + I_{fac} \cdot R_{dark}) \cdot C_s^{-1}$. G_{fac} is an empirical coefficient representing the composite sensitivity of stomata to these factors. Stomatal opening in response to PPFD is controlled via $(A + I_{fac} \cdot R_{dark})$, which gives an estimation of gross photosynthetic rate and is considered to be related to energy requirements for maintaining guard cell turgor (Falge et al., 1996). Effects of non-uniform stomatal closure ('patchiness') on stomatal conductance are not considered in this model.

Leaf internal CO_2 partial pressure is calculated from net photosynthesis and stomatal conductance according to Fick's law

$$C_i = C_s - \frac{A \cdot 1.6 \cdot 100}{g_s} \quad (10)$$

where 1.6 accounts for the difference in diffusivity between CO_2 and H_2O and the factor 100 corrects

for the difference in the units of C_s and A/g_s . Due to the fact that net photosynthesis and stomatal conductance are not independent, the model must solve for the internal CO_2 partial pressure in an iterative fashion (Harley and Tenhunen, 1991; Harley and Baldocchi, 1995).

Boundary layer conditions encountered in the cuvette during measurements (boundary layer conductance typically > 2.8 mol/m² per s) were mimicked using the equations by Nobel (1991) together with the corresponding leaf dimensions and wind speed. Air pressure at the study site was fixed at a mean value of 84 kPa.

To meet recent efforts to achieve a common model documentation within the scientific community (Benz and Knorrrenschild, 1997), we have decided to provide a documentation of the model presented in this paper using the model documentation system ECOBAS (Benz et al., 1997; Benz, submitted), which has been set up for our model in co-operation with Benz and co-workers. This documentation is freely accessible via WWW (http://dino.wiz.uni-kassel.de/model_db/mdb/ecomont.html).

3. Results

3.1. Parameterisation of the photosynthesis submodel

The parameters determining the temperature dependencies of τ were taken from Jordan and Ogren (1984), those of K_C and K_O from Badger and Collatz (1977) (Table 2). Each of the three kinetic constants is described by the Arrhenius relationship given in Eq. (8). The other four biochemical parameters R_{day} , V_{cmax} , P_{ml} and α were

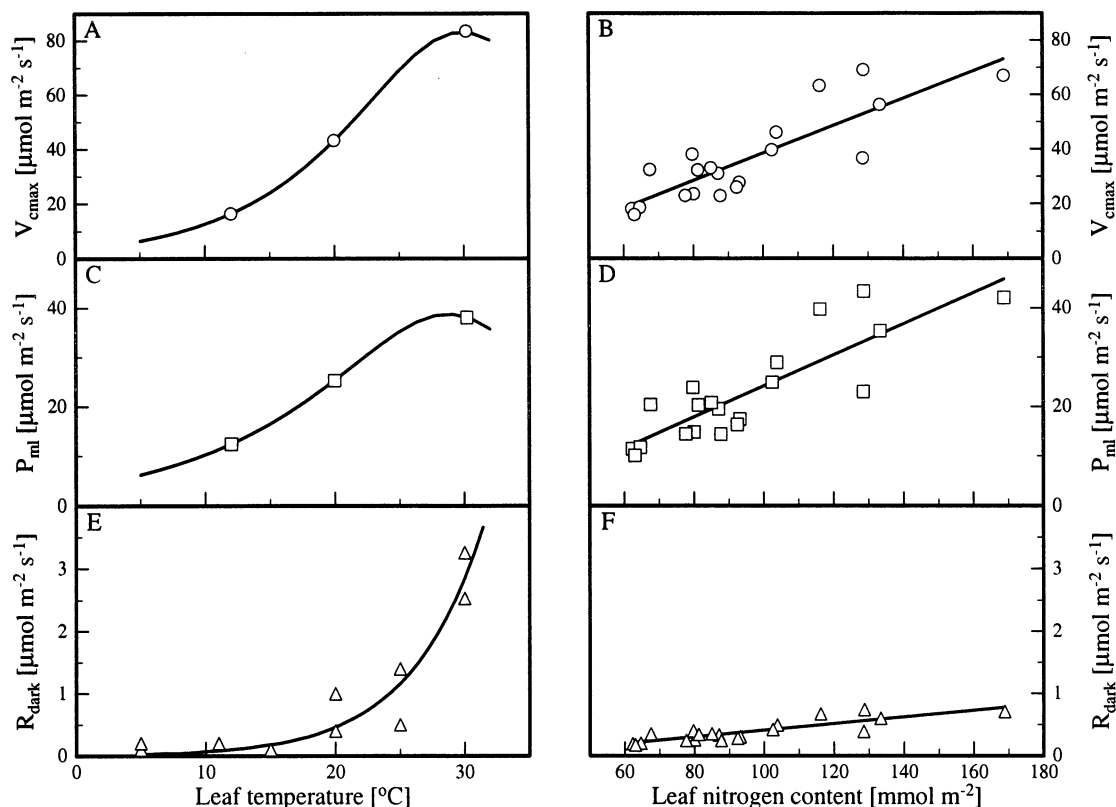


Fig. 1. Temperature and nitrogen dependency of the maximum rate of carboxylation, V_{cmax} (A and B, respectively), the potential rate of RuBP regeneration, P_{ml} (C and D, respectively) and the dark respiration rate, R_{dark} (E and F, respectively), of *D. glomerata*. Symbols represent values that were calculated from measured data, lines are model simulations. The temperature dependencies are based on a leaf nitrogen content (N_L) of 110 mmol/m², the nitrogen dependencies refer to a leaf temperature of 20°C.

estimated from A/C_i and/or light response curves as described below.

Estimates of R_{day} , the rate of respiration that continues in the light (Brooks and Farquhar, 1985), were made using a technique described by Falge et al. (1996). Estimates of dark respiration (R_{dark}) at different leaf temperatures were obtained from the y -intercept of a linear regression through data points describing the initial portion of the light response curves at different leaf temperatures. The temperature dependency of R_{dark} was then described by Eq. (8) using non-linear least-squares analysis (Table 3/A, Fig. 1/E). R_{day} was then calculated from R_{dark} using Eqs. (2), (3a) and (3b).

R_{dark} of the investigated species varied between 0.46 (*D. glomerata*) and 2.68 $\mu\text{mol}/\text{m}^2$ per s (*P.*

viviparum), most of the species' dark respiration rate ranging between 1–2 $\mu\text{mol}/\text{m}^2$ per s (Table 4).

Having fixed the temperature dependency of R_{day} , estimates of V_{cmax} were obtained by fitting data points with C_i values lower than 20 Pa from A/C_i curves to Eq. (1), with the term W_C substituted by Eq. (4), by least-squares regression technique. Similarly, estimates of P_{ml} were obtained by non-linear least-squares regression technique, fitting all data points of the A/C_i curves to Eq. (1) with the term W_J substituted by Eq. (5).

This procedure works only if measured A/C_i curves are available. For two species, *R. alec-torolophus* and *T. pratense*, this was not the case. V_{cmax} and P_{ml} of these two species were determined from light response curves at different leaf

Table 3
Parameters of the photosynthesis submodel obtained from parameterisation of measured response curves (*A*) and additional parameters needed to calculate the nitrogen dependencies of $V_{\text{cmax}}(T_{\text{ref}})$, $P_{\text{m}}(T_{\text{ref}})$ and $R_{\text{dark}}(T_{\text{ref}})$ (*B*)

<i>A</i>	Parameter	Units	Dg	Kp	Ns ^a	Pa	Pm	Pv	Po	Ra	Tm	Tp	Tf	Tc ₁₀	Tc ₅₀	Vm		
<i>V_{cmax}</i>	$V_{\text{cmax}}(T_{\text{ref}})$	$\mu\text{mol}/\text{m}^2$ per s	45.58	28.88	37.93	52.88	47.05	37.16	30.03	53.24	56.67	48.79	24.85	35.07	18.89	13.30		
	$\Delta H_A(V_{\text{cmax}})$	J/mol	88 434	149 061	61 304	64 490	79 294	60 940	57 098	60 600	118 599	53 017	54 017	68 000	68 362	102 568		
	$\Delta H_D(V_{\text{cmax}})$	J/mol	199 390	198 000	202 583	200 000	200 415	199 571	204 000	202 000	202 000	197 500	202 000	201 186	201 000	202 198	201 194	
	$\Delta S(V_{\text{cmax}})$	J/K per mol	656	656	656	656	656	656	656	656	656	656	656	656	656	656	656	
	<i>P_m</i>	$P_{\text{m}}(T_{\text{ref}})$	$\mu\text{mol}/\text{m}^2$ per s	28.57	17.51	25.29	31.18	25.61	27.85	17.48	26.71	35.38	27.03	15.36	22.93	11.97	5.57	
		$\Delta H_A(P_{\text{m}})$	J/mol	65 649	78 754	44 386	51 014	56 292	61 521	57 101	37 407	115 191	68 707	67 161	55 465	55 465	57 329	
		$\Delta H_D(P_{\text{m}})$	J/mol	195 860	200 000	196 168	197 551	198 050	192 521	199 247	201 000	191 300	199 000	199 000	194 000	199 521	198 922	198 922
		$\Delta S(P_{\text{m}})$	J/K per mol	643	643	643	643	643	643	643	643	643	643	643	643	643	643	643
	<i>R_{dark}</i>	$R_{\text{dark}}(T_{\text{ref}})$	$\mu\text{mol}/\text{m}^2$ per s	0.46	1.64	2.02	1.58	2.07	2.68	0.68	1.47	2.16	0.80	1.43	1.24	1.01	1.31	
		$\Delta H_A(R_{\text{dark}})$	J/mol	134 612	70 762	13 592	53 132	36 648	17 913	94 482	70 418	43 432	40 479	39 787	36 743	37 246	22 821	
<i>z</i>		mol CO ₂ /mol photons	0.05	0.05	0.05	0.05	0.06	0.06	0.06	0.06	0.06	0.06	0.06	0.05	0.06	0.045	0.06	
<i>B</i>	$V_{\text{cmax}}(T_{\text{ref}})$	$\mu\text{mol CO}_2/\text{mmol N per s}$	0.530	0.344	0.481	0.369	0.975	0.617	0.530	0.343	1.382	0.885	0.314	0.287	0.423	0.169		
	<i>C₀</i>	$\mu\text{mol}/\text{m}^2$ per s	-12.39	-3.02	-9.87	14.81	-32.99	-39.52	-18.42	1.82	-141.31	-70.84	1.36	3.94	3.94	-22.86	-6.44	
	<i>R_{fix}</i>	—	0.011	0.062	0.054	0.031	0.046	0.076	0.023	0.028	0.043	0.017	0.059	0.037	0.055	0.101	0.101	
	<i>P_{fix}</i>	—	0.630	0.659	0.649	0.600	0.553	0.661	0.580	0.508	0.530	0.557	0.574	0.665	0.638	0.638	0.424	

The first letters of the generic and species name are used as abbreviations. For symbols and other abbreviations refer to Appendix A (^a values refer to a surface area basis).

Table 4

Estimates of the maximum rate of carboxylation (V_{cmax}), the potential rate of RuBP regeneration (P_{ml}) and the dark respiration rate (R_{dark}) ($\mu\text{mol}/\text{m}^2$ per s) at 20°C, the temperature optima ($T_{\text{opt.}}$) of V_{cmax} and P_{ml} (°C) and slope (C_N) and y -intercept (C_0) of a linear regression relating V_{cmax} to N_L (^a values refer to a surface area basis)

Species	V_{cmax}	P_{ml}	R_{dark}	$T_{\text{opt.}}$		V_{cmax}		R^2
				V_{cmax}	P_{ml}	C_N	C_0	
<i>D. glomerata</i>	43.21	27.24	0.46	29.9	28.8	0.502	−11.74	0.73
<i>K. pyramidata</i>	26.33	17.36	1.64	33.0	36.2	0.314	−2.75	0.58
<i>N. stricta</i> ^a	37.38	24.25	2.02	32.4	27.2	0.474	−9.73	0.66
<i>P. atrata</i>	50.72	30.43	1.58	28.9	29.9	0.354	14.20	0.57
<i>P. media</i>	45.42	25.12	2.07	30.7	31.2	0.941	−31.85	0.80
<i>P. viviparum</i>	35.36	23.36	2.68	27.9	23.4	0.587	−37.61	0.74
<i>P. aurea</i>	29.79	17.27	0.68	34.1	33.1	0.526	−18.26	0.87
<i>R. alectorolophus</i>	52.26	26.55	1.47	31.5	33.6	0.336	1.78	0.65
<i>T. montanum</i>	50.65	26.86	2.16	29.5	26.0	1.235	−126.29	0.56
<i>T. pratense</i>	47.89	26.67	0.80	30.8	33.8	0.869	−69.54	0.74
<i>T. flavescens</i>	24.22	13.90	1.43	29.7	26.1	0.306	1.33	0.70
<i>T. europaeus</i> , lower leaves	34.10	22.69	1.24	30.7	33.4	0.279	3.84	0.55
<i>T. europaeus</i> , upper leaves	18.57	11.84	1.01	32.5	33.4	0.416	−22.47	0.72
<i>V. myrtilus</i>	12.96	5.49	1.31	33.7	32.6	0.164	−6.28	0.64

temperatures according to a technique described by Niinemets and Tenhunen (1997). Essential to this technique is, that light saturation of net photosynthesis is reached at an incident photon flux density at which W_C equals W_J . Thus the potential rate of RuBP regeneration may be calculated from W_C at saturating photon flux density. Estimation of V_{cmax} from light saturated photosynthesis will be described in the following section.

Repeating these procedures at different leaf temperatures, estimates of V_{cmax} and P_{ml} at these leaf temperatures were obtained. Again non-linear least-squares regression analysis was performed to fit these data to Eq. (7), obtaining the four parameters describing the temperature dependency of V_{cmax} and P_{ml} (Table 3/A, Fig. 1/A and C). Because no A/C_i curves and light response curves at leaf temperatures higher than 30°C were available, ΔS of the investigated species was fixed for both V_{cmax} and P_{ml} at values available from literature (Harley and Tenhunen (1991) for *Arbutus unedo*).

V_{cmax} and P_{ml} at 20°C (Table 4) varied considerably among the investigated species, the dwarf shrub *V. myrtilus* having the lowest and the annual *R. alectorolophus* having the highest val-

ues. The herbs, except for the lower leaves of *T. europaeus*, separated from the grasses, except for *D. glomerata*, insofar as their values of V_{cmax} and P_{ml} were higher than 29.8 and 17.3 $\mu\text{mol}/\text{m}^2$ per s, respectively. The temperature optima of V_{cmax} and P_{ml} (Table 4) ranged from 27.9 (*P. viviparum*) and 26.0 (*T. montanum*) to 34.1 (*P. aurea*) and 36.2°C (*K. pyramidata*), respectively.

Having fixed the parameters determining R_{dark} , V_{cmax} , P_{ml} and those needed for the stomatal submodel (for the parameterisation technique see below) α , the apparent quantum yield at saturating CO_2 , was adjusted to give a good fit to the initial portion of the measured light response curves (Table 3/A).

Except for the upper leaves of *T. europaeus*, which already showed visible signs of senescence and whose α had to be adjusted to 0.045 mol CO_2 mol photons^{-1} , α ranged between 0.05 and 0.06 mol CO_2 mol photons^{-1} , which is within the typical range for C_3 species, assuming a leaf absorptance of 83% (Ehleringer and Björkman, 1977).

The success of the parameterisation was assessed visually, comparing measured response curves and model output and for some species

slight adjustments (< 5%) of the model parameters were made to improve the fit of the model.

3.2. Derivation of the nitrogen dependencies of V_{cmax} , P_{ml} and R_{dark} from measurements of photosynthetic capacity

The following section deals with a technique and the underlying assumptions, which allow to derive a set of V_{cmax} , P_{ml} and R_{dark} from a single measurement of A_{max} . Since the leaves used for measurements of A_{max} were subjected to subsequent nitrogen analysis, this technique allows to derive nitrogen dependencies of V_{cmax} , P_{ml} and R_{dark} using linear regression techniques.

Following Niinemets and Tenhunen (1997) we assumed that at the present ambient CO_2 partial pressure net photosynthesis at saturating light intensity, A_{max} , is determined by RUBISCO activity. In terms of the leaf model this means that A_{max} equals Eq. (1) with W_C limiting the rate of carboxylation. To solve for R_{dark} , we followed other researchers (Farquhar et al., 1980; Nikolov et al., 1995; Pachepsky and Acock, 1996) assuming that altered leaf physiological activity is accompanied by proportional alterations in dark respiration rate, taking R_{dark} as a proportion of V_{cmax} according to

$$R_{\text{dark}} = R_{\text{fac}} \cdot V_{\text{cmax}} \quad (11)$$

where R_{fac} is a species-specific proportionality coefficient. R_{fac} , determined as the ratio between R_{dark} and V_{cmax} , of the investigated species ranged between 0.011 (*D. glomerata*) and 0.101 (*V. myrtillus*), most of the investigated species having a R_{fac} between 0.02 and 0.07 (Table 3/B).

Assuming that half of the dark respiration rate continues in the light under saturating light intensity (see Eq. (3a) and discussion), R_{day} may be expressed as

$$R_{\text{day}} = \frac{R_{\text{fac}} \cdot V_{\text{cmax}}}{2} \quad (12)$$

Combining this expression of R_{day} with Eq. (1), when W_C is limiting the rate of carboxylation and solving for V_{cmax} gives

$$V_{\text{cmax}} = \frac{A_{\text{max}}}{\left(1 - \frac{0.5 \cdot O}{\tau \cdot Ci}\right) \cdot Ci} - \frac{R_{\text{fac}}}{Ci + K_C \cdot \left(1 + \frac{O}{K_O}\right)} \quad (13)$$

In order to stay consistent with the terminology used in Eq. (7) we decided to establish the nitrogen dependency of V_{cmax} via a nitrogen dependency of $V_{\text{cmax}}(T_{\text{ref}})$, holding ΔH_a , ΔH_d and ΔS constant. Repeating this procedure for all the leaves, which were used in measurements of photosynthetic capacity and subsequently subjected to nitrogen analysis and running a regression analysis through the data points obtained thereby, we obtained a relationship of the form

$$\text{Parameter} = C_N(\text{Parameter}) \cdot N_L + C_0(\text{Parameter}) \quad (14)$$

where Parameter may be substituted for either V_{cmax} or $V_{\text{cmax}}(T_{\text{ref}})$ and $C_N(\text{Parameter})$ and $C_0(\text{Parameter})$ represent the slope and y -intercept, respectively, of the linear regression. The coefficients of determination resulting from this regression analysis, relating V_{cmax} and $V_{\text{cmax}}(T_{\text{ref}})$ to N_L , are the same, since V_{cmax} is equal to $V_{\text{cmax}}(T_{\text{ref}})$ times a constant (ΔH_a , ΔH_d and ΔS are held constant) according to Eq. (7).

The slopes of the nitrogen dependencies of V_{cmax} (Table 4) varied considerably among the investigated species, *V. myrtillus* (0.164 $\mu\text{mol CO}_2/\text{mmol N per s}$) having the lowest and *T. montanum* (1.235 $\mu\text{mol CO}_2/\text{mmol N per s}$) having the highest slope. y -Intercepts were negative, except for *P. atrata*, *R. alectorolophus*, *T. flavescens* and the lower leaves of *T. europaeus* (Table 4).

Given the relationship between V_{cmax} and R_{dark} , as expressed in Eq. (11), it is then possible to calculate $R_{\text{dark}}(T_{\text{ref}})$ from $V_{\text{cmax}}(T_{\text{ref}})$ using

$$R_{\text{dark}}(T_{\text{ref}}) = \frac{V_{\text{cmax}}(T_{\text{ref}}) \cdot R_{\text{fac}}}{1 + \exp \left[\frac{\Delta S(V_{\text{cmax}}) \cdot T_{\text{ref}} - \Delta H_d(V_{\text{cmax}})}{R \cdot T_{\text{ref}}} \right]} \quad (15)$$

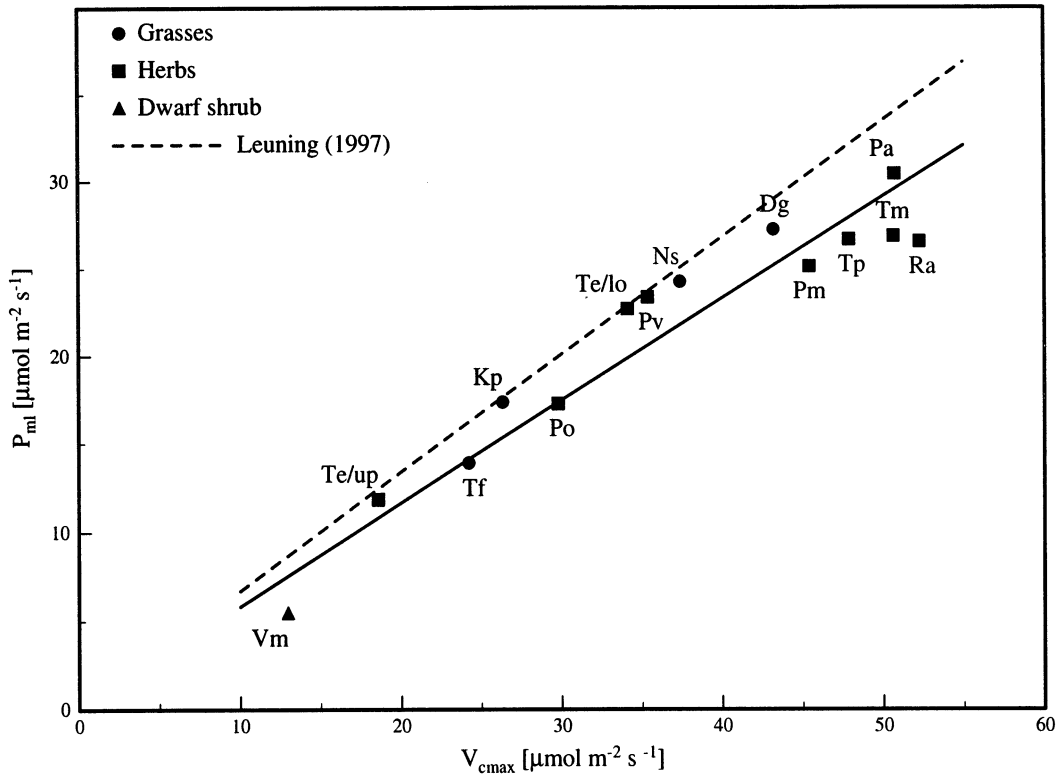


Fig. 2. Relationship between the maximum rate of carboxylation (V_{cmax}) and the potential rate of RuBP regeneration (P_{ml}) at 20°C of the investigated species. Lines represent linear regressions forced through the origin ($R^2 = 0.91$, $P < 0.002$ this study). The corresponding slopes are: 0.58 (this study) and 0.67 (Leuning 1997). The first letters of the generic and species name are used as abbreviations.

Wullschleger (1993) and Leuning (1997) showed for a great number of different species that there exists a strong correlation between V_{cmax} , the RUBISCO limited rate of carboxylation and J_{max} , the light saturated rate of electron transport. In the present paper we decided to use a species-specific ratio between P_{ml} and V_{cmax} , the so called P_{fac} (Fig. 2, Table 3/B), obtained from the parameterisation of the leaf model, using the measured response curves at 20°C leaf temperature, although the variation of the ratio between P_{ml} and V_{cmax} within the investigated species was small ($R^2 = 0.91$, $P < 0.002$, Fig. 2).

A similar procedure, as described above for R_{dark} , was used to calculate $P_{ml}(T_{ref})$ from $V_{cmax}(T_{ref})$ using

$$P_{ml}(T_{ref}) = \frac{V_{cmax}(T_{ref}) \cdot P_{fac}}{1 + \exp \left[\frac{\Delta S(V_{cmax}) \cdot T_{ref} - \Delta H_d(V_{cmax})}{R \cdot T_{ref}} \right]} \times \left(1 + \exp \left[\frac{\Delta S(P_{ml}) \cdot T_{ref} - \Delta H_d(P_{ml})}{R \cdot T_{ref}} \right] \right) \quad (16)$$

where P_{fac} is the ratio between P_{ml} and V_{cmax} at 20°C.

$R_{dark}(T_{ref})$ and $P_{ml}(T_{ref})$ thus also, although indirectly, depend on N_L , since $V_{cmax}(T_{ref})$, which is used to calculate $R_{dark}(T_{ref})$ and $P_{ml}(T_{ref})$ in Eqs. (15) and (16), depends on N_L according to Eq. (14). For the implementation of the nitrogen dependencies into the model two possibilities exist: One possibility is to use Eqs. (14)–(16), in this

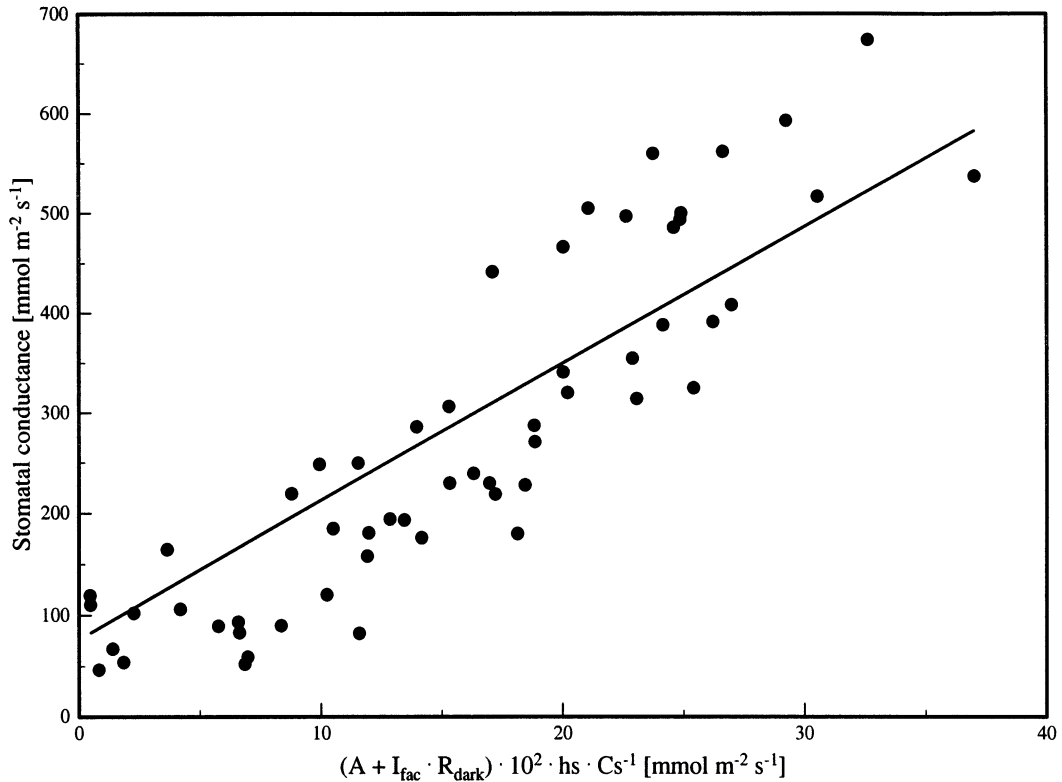


Fig. 3. Relationship between measured stomatal conductance and the product of $(A + I_{\text{fac}} \cdot R_{\text{dark}}) \cdot 10^2 \cdot h_s \cdot C_s^{-1}$ for leaves of *D. glomerata* according to Eq. (9). Data were collected episodically under the prevailing environmental conditions throughout the vegetation period 1996. Symbols are measured values, solid lines linear regressions. For values of the corresponding model parameters, G_{fac} and g_{min} , as well as the coefficients of determination refer to Table 5.

case four parameters, $C_N(V_{\text{cmax}}(T_{\text{ref}}))$, $C_0(V_{\text{cmax}}(T_{\text{ref}}))$, R_{fac} and P_{fac} , shown in Table 3/B, are needed. An alternative way is to explicitly derive nitrogen dependencies also for $R_{\text{dark}}(T_{\text{ref}})$ and $P_{\text{ml}}(T_{\text{ref}})$, using the notation as in Eq. (14). The corresponding slopes and y -intercepts can be calculated easily by multiplying $C_N(V_{\text{cmax}}(T_{\text{ref}}))$ and $C_0(V_{\text{cmax}}(T_{\text{ref}}))$ with R_{fac} and P_{fac} , respectively. Therefore we also did not include the slopes and y -intercepts of $R_{\text{dark}}(T_{\text{ref}})$ and $P_{\text{ml}}(T_{\text{ref}})$ into Table 3/B, but R_{fac} and P_{fac} instead. We favour the implementation of the nitrogen dependencies into the model in the latter form, since it keeps the model flexible enough to handle also nitrogen dependencies of V_{cmax} , P_{ml} and R_{dark} , determined in separate measurements (e.g. Anten et al., 1996), although the number of parameters involved increases from four to six, compared to the first way of implementation. An

example for the nitrogen dependencies of V_{cmax} , P_{ml} and R_{dark} is given in Fig. 1/B, D and F.

3.3. Parameterisation of the stomatal conductance submodel

The parameters G_{fac} and g_{min} from Eq. (9) were obtained by plotting the product of $(A + I_{\text{fac}} \cdot R_{\text{dark}}) \cdot 10^2 \cdot h_s \cdot C_s^{-1}$ against measured stomatal conductance, g_s , as shown for *D. glomerata* in Fig. 3. G_{fac} is obtained from the slope of a regression line going through these data points, whilst g_{min} represents the respective y -intercept. Parameters given in Table 5 are the result of pooling data from measurements of net photosynthesis and stomatal conductance under the prevailing environmental conditions, conducted episodically throughout the vegetation period 1996.

Table 5
Parameters of the stomatal conductance model according to Eq. (9)

Species	Meadow			Pasture			Abandoned area		
	G_{fac}	g_{min}	R^2	G_{fac}	g_{min}	R^2	G_{fac}	g_{min}	R^2
<i>D. glomerata</i>	13.7	76.2	0.77	—	—	—	—	—	—
<i>K. pyramidata</i>	—	—	—	10.6	22.0	0.52	—	—	—
<i>N. stricta</i> ^a	—	—	—	—	—	—	16.0	21.9	0.74
<i>P. atrata</i>	13.8	70	0.63	14.1	79.3	0.61	9.8	76.1	0.66
<i>P. media</i>	—	—	—	10.8	91.1	0.49	—	—	—
<i>P. viviparum</i>	11.9	57.0	0.63	8.9	41.2	0.75	12.0	54.5	0.46
<i>P. aurea</i>	17.0	120	0.63	10.6	74.6	0.61	24.7	130	0.70
<i>R. alectorolophus</i>	18.3	193.1	0.54	—	—	—	—	—	—
<i>T. montanum</i>	—	—	—	13.5	42.6	0.76	—	—	—
<i>T. pratense</i>	6.9	25.2	0.92	—	—	—	—	—	—
<i>T. flavescens</i>	17.0	75.4	0.60	—	—	—	—	—	—
<i>T. europaeus</i> , lower leaves	13.4	67.0	0.56	9.1	81.5	0.50	12.8	70.6	0.64
<i>T. europaeus</i> , upper leaves	19.2	29.5	0.85	9.4	32.7	0.84	20.2	94.7	0.81
<i>V. myrtillus</i>	—	—	—	—	—	—	10.5	11.7	0.74

Values given are the result of pooling gas exchange data obtained under the prevailing environmental conditions throughout the vegetation period 1996 (^a values refer to a surface area basis).

Except for *P. aurea* and *R. alectorolophus*, whose g_{min} reached 193.1 and 130.0 mmol/m² per s, respectively, g_{min} of the other species ranged between 11.7 (*V. myrtillus*) and 94.7 (upper leaves of *T. europaeus*, on the abandoned area) mmol/m² per s. G_{fac} ranged between 6.9 (*T. pratense*) and 24.7 (*P. aurea*, on the abandoned area). A smaller G_{fac} on the pasture can be observed for all the species, which occur on all three investigated sites, except for *P. atrata*.

3.4. Validation

For validation diurnal courses of net photosynthesis and stomatal conductance under the prevailing environmental conditions were used as independent data sets to validate the combined photosynthesis/stomatal conductance model. N_L of the investigated leaves was used as an input parameter, according to which the $V_{\text{cmax}}(T_{\text{ref}})$, $P_{\text{ml}}(T_{\text{ref}})$ and $R_{\text{dark}}(T_{\text{ref}})$ were calculated using the relationships given in Table 3/B. The remaining parameters were taken from Table 2 (τ , K_C and K_O), Table 3/A (α ; ΔH_a , ΔH_d and ΔS of V_{cmax} and P_{ml} ; ΔH_a of R_{dark}) and Table 5 (G_{fac} and g_{min}).

An example is given in Fig. 4, which shows a validation data set for a leaf (106 mmol/m² nitro-

gen content) of *P. atrata*. The model is capable of predicting measured net photosynthesis and stomatal conductance under the prevailing environmental conditions quite reasonably, having correlation coefficients of 0.98 and 0.68, respectively. The overall good correspondence between predicted and measured values of photosynthesis confirms the relationship between N_L and leaf parameters and the sensitivity of the model to changes in PPFD, leaf temperature and ALVPD. Predictions of stomatal conductance are of minor accuracy, overestimating stomatal conductance early in the morning and underestimating it under conditions of high irradiance in the afternoon.

3.5. Sensitivity analysis

In order to test the ability of the model to account for changes in N_L a sensitivity analysis was performed, varying N_L together with PPFD (Fig. 5/A and B), leaf temperature (Fig. 5/C and D) and CO₂ partial pressure (Fig. 5/E and F).

Increasing N_L increases V_{cmax} , which in turn causes light saturated photosynthesis in Fig. 5/A to increase. At the same time the light intensity at which saturation of net photosynthesis occurs, shifts to higher values due to the fact that P_{ml} is increased proportionally with V_{cmax} . Increasing

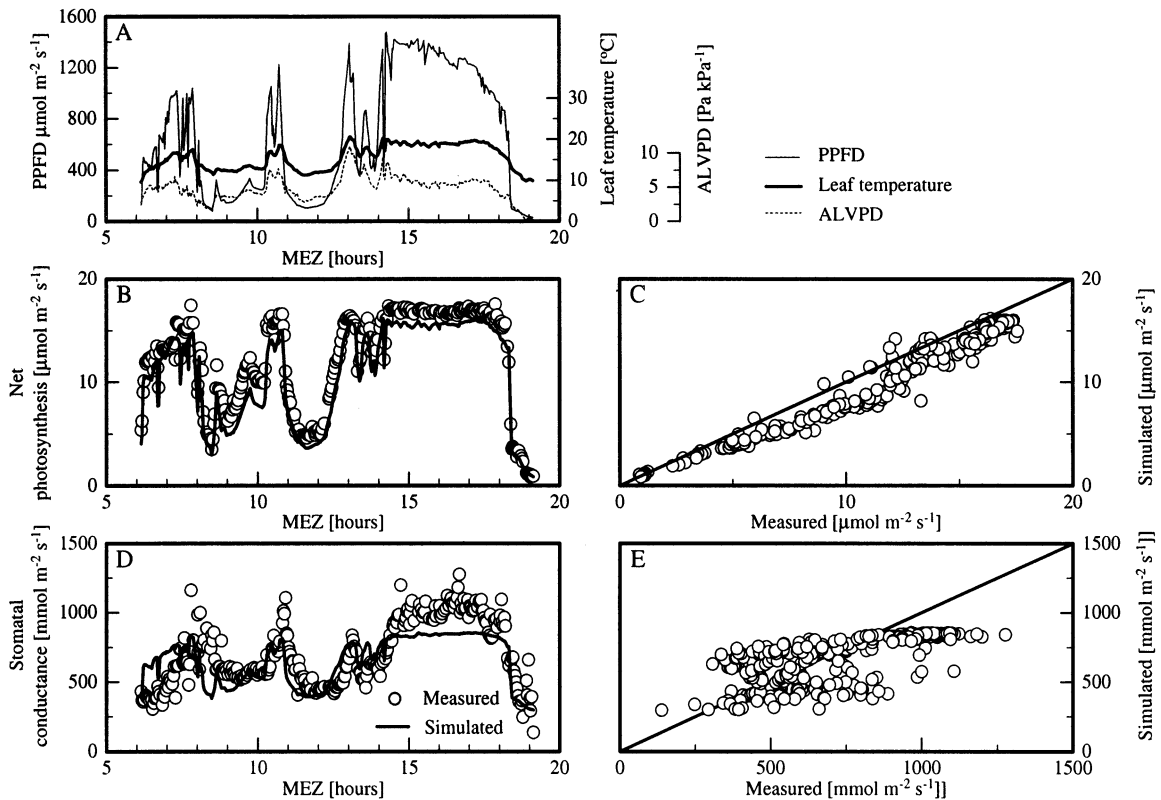


Fig. 4. Diurnal time course of photosynthetically active radiation (PPFD), leaf temperature, air to leaf vapour pressure difference (ALVPD) (A), net photosynthesis (B) and stomatal conductance (D) and comparison of measured versus simulated values of net photosynthesis (C) and stomatal conductance (E) of *P. atrata* on 10 July 1997. Solid lines are model simulations, symbols represent measured values (B and D). The correlation coefficients are 0.98 (C) and 0.68 (E).

V_{cmax} also leads to a proportional increase in R_{day} , which causes the highest light saturated photosynthesis rates to be associated with the highest dark respiration rates.

Since V_{cmax} , P_{ml} and R_{day} change in a proportional manner, the temperature optimum of net photosynthesis does not change with varying N_{L} . The benefits of increasing N_{L} on net photosynthesis rate are much more pronounced near the temperature optimum, than at very high or low temperatures. (Fig. 5/C).

The shape of the curves in Fig. 5/E, showing a proportional increase in carboxylation efficiency (CE) and CO_2 saturated photosynthesis with increasing N_{L} , again reflects the effects of balanced changes of V_{cmax} and P_{ml} . As a conse-

quence of the proportional increase in V_{cmax} and R_{day} , the CO_2 compensation point remains unaffected (Leuning et al., 1995; De Pury and Farquhar, 1997).

No general differences in model behaviour between *P. atrata*, parameterised from A/C_i curves and *T. pratense*, parameterised from light response curves, become apparent from Fig. 5. The higher gains in net photosynthesis due to increasing N_{L} of *T. pratense* must be attributed to a steeper slope of the nitrogen dependencies of V_{cmax} , P_{ml} and R_{dark} compared with those of *P. atrata* (Table 3/B).

N_{L} influences the simulated stomatal conductance only indirectly via the rate of net photosynthesis (Fig. 5/B, D and F).

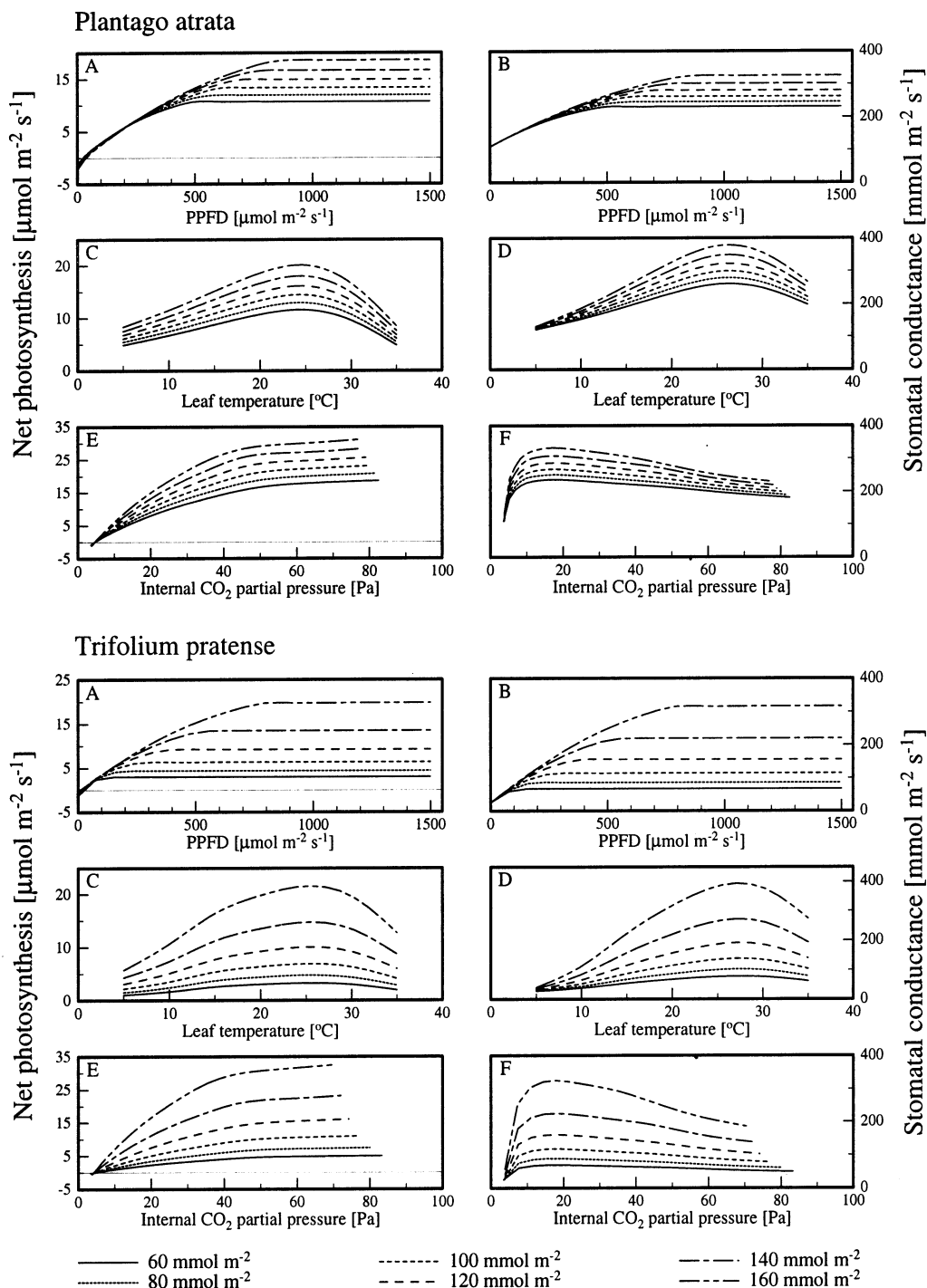


Fig. 5. Sensitivity analysis of the combined photosynthesis/stomatal conductance model showing the response of net photosynthesis (A, C and E) and stomatal conductance (B, D and F) of *P. atrata* (top) and *T. pratense* (bottom) to changes in leaf nitrogen content (N_L). Simulations assumed at a photosynthetic photon flux density (PPFD) of 1500 $\mu\text{mol}/\text{m}^2$ per s (except for A and B), a leaf temperature of 20°C (except for C and D), a CO_2 partial pressure of 35 Pa (except for E and F) and an air to leaf vapour pressure difference (ALVPD) of 9.2 Pa/kPa.

4. Discussion

The model presented in this paper was successful in predicting gas exchange response to PPFD, leaf temperature, CO_2 partial pressure, ALVPD and N_L , although the approach chosen to account for effects of N_L on gas exchange is rather a phenomenological one, compared with more process-oriented approaches, like the one presented recently by Niinemets and Tenhunen (1997). However, the shortcoming of these more process-oriented approaches is, that the number of parameters that need to be determined, increases considerably and some of these parameters (e.g. chlorophyll content) are not being investigated routinely in field studies of gas exchange. The shortcomings of our approach must thus be evaluated in terms of the overall goals of the present study. The main aim was to provide the physiological data basis for an up-scaling study at the Monte Bondone research area (Cernusca et al., 1998, this issue). Since the investigated sites are characterised by a high diversity of plant species, it was necessary to obtain data sets on gas exchange of as many species as possible. In consequence 13 key species, selected according to their abundance and contribution to stand biomass on the different sites, were identified, their gas exchange characteristics studied and leaf models parameterised for each species. The high number of investigated species makes this data set unique not only for semi-natural mountain ecosystems. As far as we know from literature, there are only few other studies (e.g. Tenhunen et al., 1995) where as many species of the same ecosystem have been characterised in terms of leaf model parameters.

The model is based on a heterogeneous, though firm data basis and reproduces general characteristics of the gas exchange of C_3 plants very well, as shown by the sensitivity tests in Fig. 5 and the validation in Fig. 4. Key features of the model are that respiratory costs for leaf maintenance scale directly with leaf physiological activity (Walters and Field, 1987; Ceulemans and Saugier, 1991) and that V_{cmax} is correlated to P_{ml} at a reference temperature (Leuning, 1997). The remarkable small scatter in a data set containing 109 different

species (Wullschleger, 1993; Leuning, 1997) of the relationship between V_{cmax} and J_{max} has encouraged other modellers (Leuning et al., 1995; De Pury and Farquhar, 1997) to use this relationship to estimate J_{max} from V_{cmax} . Recent findings although show that adaptation to growth irradiance may shift the balance between RUBISCO activity (V_{cmax}) and electron transport (J_{max} , respectively, P_{ml}) (Sukenic et al., 1987; Ögren, 1993; Hikosaka and Terashima, 1996). In the present paper, due to the lack of corresponding data, the latter results were ignored and a fixed ratio between these two processes was assumed, as in Leuning et al. (1995) and De Pury and Farquhar (1997). Although no significant differences ($P < 0.072$) between our data and the fit obtained by Leuning (1997) were observed, we decided not to use the ratio found by Leuning (1997), but a more accurate, species-specific ratio, derived directly from our data (Table 3/B).

Since no response curves at leaf temperatures higher than 30°C were available we decided to hold ΔS for both V_{cmax} and P_{ml} constant at the values determined for *A. unedo* by Harley and Tenhunen (1991). The same approach has been applied successfully to *Picea abies* by Falge et al. (1996), though further studies need to be conducted, investigating whether data from the Mediterranean shrub *A. unedo* may be applied to herbaceous mountain species. As a consequence the model cannot be applied with confidence at temperatures exceeding 30°C .

Niinemets and Tenhunen (1997) reviewed several studies for R_{fac} , the ratio between R_{dark} and V_{cmax} and found 0.065 to be a suitable mean value. R_{fac} of the investigated species, except for *V. myrtillus*, ranges between 0.011 and 0.076 (Table 3/B) with a mean value of 0.042, thus the value given in Niinemets and Tenhunen (1997) being within the range of our measurements.

In the model it is assumed that half of the dark respiration rate continues in the light (Eq. (3a)), unless PPFD drops below $25 \mu\text{mol}/\text{m}^2$ per s. In the latter case inhibition of R_{dark} is increased from 0.5 at $25 \mu\text{mol}/\text{m}^2$ per s to 1 at darkness, according to Eq. (3b). Within this PPFD range the model behaviour corresponds well with the results of Brooks and Farquhar (1985), although they

found the ratio to be 0.2 at saturating light intensities. Other researchers found the ratio $R_{\text{day}}/R_{\text{dark}}$ to be 0.8 (McCashin et al., 1988) or even nearly 1 (Azcòn-Bieto and Osmond, 1983). In the absence of a clear understanding of the extent to which R_{dark} is really inhibited in light, we thus feel, in accordance with Falge et al. (1996), that assuming a mean value of 0.5 for PPFD values higher than $25 \mu\text{mol}/\text{m}^2 \text{ per s}$ is a reasonable approach.

As far as the V_{cmax} versus N_L relationship is concerned, we know of only few other studies (e.g. Field, 1983; Harley et al., 1992; Anten et al., 1996), that quantify this relationship (although in none of the cited references V_{cmax} was calculated at 20°C , as in this study). The slopes given by these authors range from $0.839 \mu\text{mol}/\text{mmol N per s}$ (at 29°C) for sun leaves of *Gossypium hirsutum* (Harley et al., 1992) to $0.282 \mu\text{mol}/\text{mmol N per s}$ (at 23°C) for shade leaves of *Tetrorchidium rubrivinium* (Anten et al., 1996). Again the dwarf shrub *V. myrtillus* is isolated from the herbaceous species having the lowest slope, indicating a rather inefficient use of N_L , not even reaching the slope of the shade species *T. rubrivinium* (Anten et al., 1996). Three species, *P. media*, a species with highly efficient oriented sun leaves, *T. montanum* and *T. pratense*, two species profiting from nitrogen-fixing bacteria associated with their roots, exceed the range given in literature, having slopes greater than $0.839 \mu\text{mol}/\text{mmol N per s}$.

In the absence of a mechanistic description of stomatal functioning researchers have to refer to empirical or so-called semi-empirical models of stomatal functioning. Among those available, the model proposed by Ball et al. (1987) is one of the most frequently used (for a summary of the different approaches we refer to Friend, 1995), although this model caused concern, because it is widely accepted that stomata respond to humidity deficit rather than to leaf surface relative humidity (Aphalo and Jarvis, 1991), which led Leuning (1995) to replace surface relative humidity with a hyperbolic function of humidity deficit. Since by using this modified model by Leuning no obvious differences in the modelling results were obtained (data not shown), we decided to use the simpler model Ball et al. (1987), incorporating the modifications proposed by Falge et al. (1996).

Sala and Tenhunen (1996) showed for *Quercus ilex* in a Mediterranean watershed, that G_{fac} is closely related to predawn leaf water potential and thus to soil water status, decreasing during periods of decreased water availability. In the present study not enough data relating G_{fac} to parameters of soil water status were available, which would allow to scale G_{fac} from day to day according to alterations in soil water status. Therefore all available data were pooled to determine an average G_{fac} value over the whole vegetation period for each study site. Since precipitation is abundant at the study site during the whole vegetation period and soil water potential falls below critical values rather rarely (unpublished data), this means that stomatal conductance would be overestimated using these average values of G_{fac} during seldom periods of water shortage.

5. Conclusion

In the present paper a combined experimental and modelling approach, centred on the intimate relationship between leaf nitrogen content and photosynthesis is presented and applied to 13 key species from three differently managed mountain grassland ecosystems. The present data set is unique for the ecosystems investigated and presents the basis for scaling up gas exchange from the leaf to the whole plant and canopy level and further to the landscape level at the research area Monte Bondone. The present data set also serves as a basis for future studies, insofar, as it may be used to reduce experimental effort when deriving key parameters of gas exchange for an assessment of the functional biodiversity of the investigated ecosystems.

Acknowledgements

This work was conducted within the EU-STEP-project INTEGRALP, co-ordinated by ICALPE/France and the EU-TERI-project ECOMONT (Project No. ENV4-CT95-0179), co-ordinated by Alexander Cernusca, University of Innsbruck/Austria. The Centro di Ecologia Alpina and the

Servizio Parchi e Foreste Demaniali (both Trento/Italy) are gratefully acknowledged for their logistic support, as well as Eva Schwarz, who carried out a part of the field work and Cor Zonnefeld for his critical comments on the temperature dependencies of the model parameters. Special thank is due to Joachim Benz, who kindly set up the ECOBAS documentation of our model and provided valuable comments on an earlier version of the manuscript.

Appendix A. Symbols and abbreviations

A	net photosynthesis ($\mu\text{mol}/\text{m}^2$ per s)	J_{max}	maximum electron transport capacity (μmol electrons m^2 per s)
ALVPD	air to leave vapour pressure difference (Pa/kPa)	k	slope of the linear relationship between I_{fac} and PPFD in the PPFD range from 0–25 $\mu\text{mol}/\text{m}^2$ per s (m^2 s/ μmol)
A_{max}	photosynthetic capacity ($\mu\text{mol}/\text{m}^2$ per s)	K_{C}	Michaelis–Menten constant for carboxylation (Pa)
CE	carboxylation efficiency ($\mu\text{mol}/\text{m}^2$ per s per Pa)	$K_{\text{C}}(T_{\text{ref}})$	Michaelis–Menten constant for carboxylation at the reference temperature of 293.16 K (Pa)
C_0	y -intercept of the linear relationship between model parameters and leaf nitrogen content ($\mu\text{mol}/\text{m}^2$ per s)	K_{O}	Michaelis–Menten constant for oxygenation (Pa)
C_i	internal CO_2 partial pressure (Pa)	$K_{\text{O}}(T_{\text{ref}})$	Michaelis–Menten constant for oxygenation at the reference temperature of 293.16 K (Pa)
C_{N}	slope of the linear relationship between model parameters and leaf nitrogen content (μmol CO_2 /mmol N per s)	N_{L}	leaf nitrogen content (mmol/ m^2)
C_{S}	leaf surface CO_2 partial pressure (Pa)	O	internal O_2 partial pressure (Pa)
d	y -intercept of the linear relationship between I_{fac} and PPFD in the PPFD range from 0–25 $\mu\text{mol}/\text{m}^2$ per s (–)	P_i	inorganic phosphate
G_{fac}	stomatal sensitivity coefficient (–)	P_{fac}	ratio between P_{ml} and V_{cmax} at 20°C leaf temperature (–)
g_{min}	minimum stomatal conductance (mmol/ m^2 per s)	P_{m}	CO_2 saturated photosynthesis rate at any given irradiance and temperature ($\mu\text{mol}/\text{m}^2$ per s)
g_{s}	stomatal conductance (mmol/ m^2 per s)	P_{ml}	potential rate of RuBP regeneration ($\mu\text{mol}/\text{m}^2$ per s)
hs	leaf surface relative humidity (–)	$P_{\text{ml}}(T_{\text{ref}})$	potential rate of RuBP regeneration at the reference temperature of 293.16 K in the absence of any deactivation due to high temperature ($\mu\text{mol}/\text{m}^2$ per s)
I_{fac}	coefficient representing the extent to which dark respiration is inhibited in the light (–)	PPFD	photosynthetic photon flux density ($\mu\text{mol}/\text{m}^2$ per s)
		R	gas constant (8.314 m^3 Pa/mol per K)
		R_{dark}	dark respiration rate ($\mu\text{mol}/\text{m}^2$ per s)
		$R_{\text{dark}}(T_{\text{ref}})$	dark respiration rate at the reference temperature of 293.16 K ($\mu\text{mol}/\text{m}^2$ per s)

R_{day}	respiration rate from processes other than photorespiration ($\mu\text{mol}/\text{m}^2$ per s)
R_{fac}	ratio between R_{dark} and V_{cmax} at 20°C leaf temperature (—)
RUBISCO	ribulose-1,5-bisphosphate carboxylase/oxygenase
RuBP	ribulose-1,5-bisphosphate
T_{K}	leaf temperature (K)
T_{opt}	temperature optimum (°C)
V_{cmax}	maximum rate of carboxylation ($\mu\text{mol}/\text{m}^2$ per s)
$V_{\text{cmax}}(T_{\text{ref}})$	maximum rate of carboxylation at the reference temperature of 293.16 K in the absence of any deactivation due to high temperature ($\mu\text{mol}/\text{m}^2$ per s)
W_{C}	RUBISCO limited rate of carboxylation ($\mu\text{mol}/\text{m}^2$ per s)
W_{J}	RuBP limited rate of carboxylation, when RuBP regeneration is limited by electron transport ($\mu\text{mol}/\text{m}^2$ per s)
W_{P}	RuBP limited rate of carboxylation, when RuBP regeneration is limited by inorganic phosphate ($\mu\text{mol}/\text{m}^2$ per s)
α	apparent quantum yield of net photosynthesis at saturating CO_2 (mol CO_2 /mol photons)
ΔH_{a}	energy of activation (J/mol)
ΔH_{d}	energy of deactivation (J/mol)
ΔS	entropy term (J/K per mol)
τ	RUBISCO specificity factor (—)
$\tau(T_{\text{ref}})$	RUBISCO specificity factor at the reference temperature of 293.16 K (—)

References

- Anten, N.P.R., Hernandez, R., Medina, E.M., 1996. The photosynthetic capacity and nitrogen concentration as related to light regime in shade leaves of a montane tropical forest tree, *Tetrorchidium rubrivenium*. *Func. Ecol.* 10, 491–500.
- Aphalo, P.J., Jarvis, P.G., 1991. Do stomata respond to relative humidity? *Plant Cell Environ.* 14, 127–132.
- Azcón-Bieto, J., Osmond, C.B., 1983. Relationship between photosynthesis and respiration. The effect of carbohydrate status on the rate of CO_2 production by respiration in darkened and illuminated wheat leaves. *Plant Physiol.* 71, 574–581.
- Badger, M.R., Collatz, G.J., 1977. Studies on the kinetic mechanism of ribulose-1,5-bisphosphate carboxylase and oxygenase reactions, with particular reference to the effect of temperature on kinetic parameters. *Yearbook Carnegie Inst. Washington* 76, 355–361.
- Bahn, M., Cernusca, A., 1998. Effects of land-use changes on plants—a functional approach. In: Cernusca, A., U. Tappeiner (Editors), *ECOMONT-Ecological effects of land-use changes on European terrestrial mountain ecosystems*. Blackwell, in press.
- Bahn, M., Cernusca, A., Tappeiner, U., Tasser, E., 1994. Wachstum krautiger Arten auf einer Mähwiese und einer Almbrache. *Ver. Ges. Ökol.* 23, 23–30.
- Baldocchi, D.D., 1993. Scaling water vapor and carbon dioxide exchange from leaves to canopy: rules and tools. In: Ehleringer, J.R., Field, C.B. (Eds.), *Scaling Physiological Processes: Leaf to Globe*. Academic Press, San Diego, pp. 77–116.
- Ball, J.T., Woodrow, I.E., Berry, J.A., 1987. A model predicting stomatal conductance and its contribution to the control of photosynthesis under different environmental conditions. In: Biggens, J. (Ed.), *Progress in Photosynthesis Research*, vol. IV, Proceedings of the Seventh International Congress on Photosynthesis. Martinus Nijhoff, Dordrecht, pp. 221–224.
- Bassow, S.L., Bazzaz, F.A., 1997. Intra- and inter-specific variation in canopy photosynthesis in a mixed deciduous forest. *Oecologia* 109, 507–515.
- Benz, J., Knorrnschild, M., 1997. Call for a common model documentation etiquette. *Ecol. Model.* 97, 141–143.
- Benz, J., Hoch, T., Gabel, T., 1997. Documentation of Mathematical Models in Ecology—an unpopular task? *Newslett. Int. Soc. Ecol. Model. (ECOMOD)* December, 1–7.
- Brooks, A., Farquhar, G.D., 1985. Effect of temperature on the CO_2/O_2 specificity of ribulose-1,5-bisphosphate carboxylase/oxygenase and the rate of respiration in the light: estimates from gas-exchange experiments on spinach. *Planta* 165, 397–406.
- Cernusca, A., Tappeiner, U., Agostini, A., Bahn, M., Bezzi, A., Egger, R., Kofler, R., Newsely, C., Orlandi, D., Prock, S., Schatz, H., Schatz, I., 1992. Ecosystem research on mixed grassland/woodland ecosystems. First results of the EC-STEP-project INTEGRALP on Mt. Bondone. *Studi. Trent. Sci. Nat. Acta Biol.* 67, 99–133.
- Cernusca, A., Tappeiner, U., Bahn, M., Bayfield, N., Chemini, C., Fillat, F., Graber, W., Rosset, M., Siegwolf, R., Tenhunen, J., 1996. *ECOMONT—Ecological effects of land-use changes on European terrestrial mountain ecosystems*. *Pirineos* 147–148, 145–172.
- Cernusca, A., Bahn, M., Chemini, C., Graber, W., Siegwolf, R., Tappeiner, U., Tenhunen, J. (1998). *ECOMONT: a combined approach of field measurements and process-*

- based modelling for assessing effects of land-use in mountain landscapes. *Ecol. Model.* 113, 167–178.
- Ceulemans, R.J., Saugier, B., 1991. Photosynthesis. In: Raghavendra, A.S. (Ed.), *Physiology of Trees*. Wiley, New York, pp. 21–50.
- Chapin III, F.S., 1980. The mineral nutrition of wild plants. *Ann. Rev. Ecol. Syst.* 11, 233–260.
- De Pury, D.G.G., Farquhar, G.D., 1997. Simple scaling of photosynthesis from leaves to canopies without the errors of big-leaf models. *Plant Cell Environ.* 20, 537–557.
- Ehleringer, J., Björkman, O., 1977. Quantum yields for CO₂ uptake in C₃ and C₄ plants: dependence on temperature, CO₂ and O₂ concentration. *Plant Physiol.* 59, 86–90.
- Evans, J.R., 1989. Photosynthesis and nitrogen relationships in leaves of C₃ plants. *Oecologia* 78, 9–19.
- Falge, E., Graber, W., Siegwolf, R., Tenhunen, J.D., 1996. A model of the gas exchange of *Picea abies* to habitat conditions. *Trees* 10, 277–287.
- Farquhar, G.D., von Caemmerer, S., 1982. Modeling photosynthetic response to environmental conditions. In: Lange, O.L., Nobel, P.S., Osmond, C.B., Ziegler H. (Eds.), *Physiological Plant Ecology*, vol. II, *Encyclopedia of Plant Physiology* 12B, Springer, Berlin, pp. 549–588.
- Farquhar, G.D., von Caemmerer, S., Berry, J.A., 1980. A biochemical model of photosynthetic CO₂ assimilation in leaves of C₃ species. *Planta* 149, 78–90.
- Field, C.B., 1983. Ecological scaling of carbon gain to stress and resource availability. In: Mooney, H.A., Winner, W.E., Pell, E.J. (Eds.), *Response of Plants to Multiple Stresses. Physiological Ecology: a Series of Monographs, Texts and Treatises*. Academic Press, San Diego, pp. 35–65.
- Field, C., Mooney, H.A., 1986. The photosynthesis–nitrogen relationship in wild plants. In: T.J. Givinish (Ed.), *On the economy of plant form and function. Proceedings of the Sixth Maria Moors Cabot Symposium, 'Evolutionary constraints on primary productivity: adaptive patterns of energy capture in plants'*, Harvard Forest, August 1983. Cambridge University Press, Cambridge, MA, pp. 25–55.
- Friend, A.D., 1995. PGEN: an integrated model of leaf photosynthesis, transpiration and conductance. *Ecol. Model.* 77, 233–255.
- Gandolfo, C., Sulli, M., 1993. Studi sul clima del Trentino per ricerche dendroclimatologiche e di ecologia forestale. Provincia Autonoma di Trento-Servizio Foreste, Caccia e Pesca, pp. 83.
- Harley, P.C., Baldocchi, D.D., 1995. Scaling carbon dioxide and water vapour exchange from leaf to canopy in a deciduous forest. I. Leaf model parameterisation. *Plant Cell Environ.* 18, 1146–1156.
- Harley, P.C., Tenhunen, J.D., 1991. Modeling the photosynthetic response of C₃ leaves to environmental factors. In: K.J. Boote, R.S. Loomis (Eds.), *Modeling Crop Photosynthesis—From Biochemistry to Canopy*. CSSA Special Publication no. 19. American Society of Agronomy and Crop Science Society of America, Madison, USA, pp. 17–39.
- Harley, P.C., Thomas, R.B., Reynolds, J.F., Strain, B.R., 1992. Modelling photosynthesis of cotton grown under elevated CO₂. *Plant Cell Environ.* 15, 271–282.
- Hikosaka, K., Terashima, I., 1996. Nitrogen partitioning among photosynthetic components and its consequences in sun and shade plants. *Func. Ecol.* 10, 335–343.
- Johnson, F., Eyring, H., Williams, R., 1942. The nature of enzyme inhibitions in bacterial luminescence: sulfanilamide, urethane, temperature and pressure. *J. Cell Comp. Physiol.* 20, 247–268.
- Jordan, D.B., Ögren, W.L., 1984. The CO₂/O₂ specificity of ribulose-1,5-bisphosphate carboxylase/oxygenase. Dependence on ribulose-bisphosphate concentration, pH and temperature. *Planta* 161, 308–313.
- Leuning, R., 1995. A critical appraisal of a combined stomatal-photosynthesis model for C₃ plants. *Plant Cell Environ.* 18, 339–355.
- Leuning, R., 1997. Scaling to a common temperature improves the correlation between the photosynthesis parameters J_{max} and V_{cmax} . *J. Exp. Bot.* 48, 345–347.
- Leuning, R., Kelliher, F.M., De Pury, D.G.G., Schulze, E.D., 1995. Leaf nitrogen, photosynthesis, conductance and transpiration: scaling from leaves to canopies. *Plant Cell Environ.* 18, 1183–1200.
- McCashin, B.G., Cossins, E.A., Calvin, D.T., 1988. Dark respiration during photosynthesis in wheat leaf slices. *Plant Physiol.* 87, 155–161.
- Mooney, H.A., Field, C., Gulmon, S.L., Bazzaz, F.A., 1981. Photosynthetic capacity in relation to leaf position in desert versus old-field annuals. *Oecologia* 50, 109–112.
- Niinemets, Ü., Tenhunen, J.D., 1997. A model separating leaf structural and physiological effects on carbon gain along light gradients for the shade-tolerant species *Acer saccharum*. *Plant Cell Environ.* 20, 845–866.
- Nikolov, N.T., Massman, W.J., Schoettle, A.W., 1995. Coupling biochemical and biophysical processes at the leaf level: an equilibrium photosynthesis model for leaves of C₃ plants. *Ecol. Model.* 80, 205–235.
- Nobel, P.S., 1991. *Physicochemical and Environmental Plant Physiology*. Academic Press, San Diego, p. 635.
- Ögren, E., 1993. Convexity of the photosynthetic light-response curve in relation to intensity and direction of light during growth. *Plant Physiol.* 101, 1013–1019.
- Ögren, E., Evans, J.R., 1993. Photosynthetic light-response curves. 1. The influence of CO₂ partial pressure and leaf inversion. *Planta* 189, 182–190.
- Pachepsky, L.B., Acock, B., 1996. A model 2DLEAF of leaf gas exchange: development, validation and ecological application. *Ecol. Model.* 93, 1–18.
- Pedrotti, F., 1995. Carta della vegetazione delle Viote del Monte Bondone (Trento). Centro di Ecologia Alpina, Report No. 6.
- Reynolds, J.F., Tenhunen, J.D., Leadley, P.W., Li, H., Moorhead, D.L., Ostendorf, B., Chapin III, F.S., 1996. Patch and landscape models of arctic tundra: potentials and limitation. In: Reynolds, J.F., Tenhunen, J.D. (Eds.), *Landscape Function and Disturbance in Arctic Tundra*. Ecological Studies, vol. 120. Springer, Berlin, pp. 293–324.

- Sala, A., Tenhunen, J.D., 1996. Simulations of canopy net photosynthesis and transpiration in *Quercus ilex* L. under the influence of seasonal drought. *Agric. For. Meteorol.* 78, 203–222.
- Sharkey, T.D., 1985. Photosynthesis in intact leaves of C_3 plants: physics, physiology and limitations. *Bot. Rev.* 51, 53–105.
- Smith, E., 1937. The influence of light and carbon dioxide on photosynthesis. *Gen. Physiol.* 20, 807–830.
- Sukenik, A., Bennett, J., Falkowski, O., 1987. Light-saturated photosynthesis-limitation by electron transport or carbon fixation? *Biochem. Biophys. Acta* 891, 205–215.
- Tappeiner, U., Cernusca, A., 1994. Bestandesstruktur, Energiehaushalt und Bodenatmung einer Mähwiese, einer Almweide und einer Almbrache. *Ver. Ges. Ökol.* 23, 49–56.
- Tappeiner, U., Tasser, E., Tappeiner, G., (1998). Modelling vegetarian patterns using natural and anthropogenic influence (land use) factors: preliminary experience with a GIS based model applied to an Alpine area. *Ecol. Model.* 113, 225–237.
- Tasser, E., Prock, S., Mulser, J., 1998. The impact of land-use on the vegetation in mountain regions. In: A. Cernusca, U. Tappeiner (Eds.), *ECOMONT-Ecological effects of land-use changes on European terrestrial mountain ecosystems*. Blackwell, in press.
- Tenhunen, J.D., Siegwolf, R.T.W., Oberbauer, S.F., 1995. Effects of phenology, physiology and gradients in community composition, structure and microclimate on tundra ecosystem CO_2 exchange. In: Schulze, E.D., Caldwell, M.M. (Eds.), *Ecophysiology of Photosynthesis*. Springer, Berlin, pp. 431–460.
- Tilman, D., 1988. *Plant Strategies and the Dynamics and Structure of Plant Community*. Princeton University Press, Princeton.
- Tilman, D., 1994. Community diversity and succession: The roles of competition, dispersal and habitat modification. In: E.D. Schulze, H.A. Mooney (Eds.), *Biodiversity and Ecosystem Function*. *Ecol. Stud.*, 99, 327–346.
- Von Caemmerer, S., Farquhar, G.D., 1981. Some relationship between the biochemistry of photosynthesis and the gas exchange of leaves. *Planta* 153, 376–387.
- Walters, M.B., Field, C.B., 1987. Photosynthetic light acclimation in two rainforest *Piper* species with different ecological amplitudes. *Oecologia* 72, 449–456.
- Wullschleger, S.D., 1993. Biochemical limitations to carbon assimilation in C_3 plants—a retrospective analysis of the A/C_i curves from 109 species. *J. Exp. Bot.* 44, 907–920.